DOI: 10.1002/anie.201300519

Carbon Dots

Highly Photoluminescent Carbon Dots for Multicolor Patterning, Sensors, and Bioimaging**

*Shoujun Zhu, Qingnan Meng, Lei Wang, Junhu Zhang, Yubin Song, Han Jin, Kai Zhang, Hongchen Sun, Haiyu Wang, and Bai Yang**

Fluorescent carbon-based materials have drawn increasing attention in recent years owing to exceptional advantages such as high optical absorptivity, chemical stability, biocompatibility, and low toxicity.[1] These materials primarily include carbon dots (CDs),[2–11] nanodiamonds,[12] carbon nanotubes,[13] fullerene,[14] and fluorescent graphene.[15–21] The superior properties of fluorescent carbon-based materials distinguish them from traditional fluorescent materials, and make them promising candidates for numerous exciting applications, such as bioimaging,[2,16] medical diagnosis,[11] catalysis,[9,18] and photovoltaic devices.[19–21] Among all of these materials, CDs have drawn the most extensive notice, owing to their early discovery and adjustable parameters.[1] However, many scientific issues with CDs still await further investigation. Currently, a broad series of methods for obtaining CD-based materials have been developed,[22–31] but efficient one-step strategies for the fabrication of CDs on a large scale are still a challenge in this field. Current synthetic methods are mainly deficient in accurate control of lateral dimensions and the resulting surface chemistry, as well as in obtaining fluorescent materials with high quantum yields (QY). Moreover, it is important to expand these kinds of materials to novel applications.[22–24] Herein, a facile and high-output strategy for the fabrication of CDs, which is suitable for industrial-scale production (yield is ca. 58%), is discussed. The QY was as high as ca. 80%, which is the highest value recorded for fluorescent carbon-based materials, and is almost equal to fluorescent dyes. The polymer-like CDs were converted into carbogenic CDs by a change from low to high synthesis temperature. The photoluminescence (PL) mechanism (high QY/PL quenching) was investigated in detail by ultrafast spectroscopy. The CDs were applied as printing ink on the macro/micro scale and nanocomposites were also prepared by polymerizing CDs with certain polymers. Additionally, the CDs could be utilized as a biosensor reagent for the detection of Fe^{3+} in biosystems.

The CDs were prepared by a hydrothermal method, which is described in the Supporting Information (Figure 1a; see also the Supporting Information, Figure S1). The reaction was conducted by first condensing citric acid and ethylenediamine, whereupon they formed polymer-like CDs, which were then carbonized to form the CDs. The morphology and structure of CDs were confirmed by analysis. Figure 1b shows transmission electron microscopy (TEM) images of the CDs, which can be seen to have a uniform dispersion without apparent aggregation and particle diameters of 2–6 nm. The sizes of CDs were also measured by atomic force microscopy (AFM; Figure S2), and the average height was 2.81 nm. From the high-resolution TEM, most particles are observed to be amorphous carbon particles without any lattices; rare particles possess well-resolved lattice fringes.[22] With such a low carbon-lattice-structure content, no obvious D or G bands were detected in the Raman spectra of the CDs (Figure S3). The XRD patterns of the CDs (Figure 1c) also displayed a broad peak centered at 25° (0.34 nm), which is also attributed to highly disordered carbon atoms.[23] Moreover, NMR spectroscopy (^{1}H and ^{13}C) was employed to distinguish sp^{3}-hybridized carbon atoms from sp^{2}-hybridized carbon atoms (Figure S4). In the ^{1}H NMR spectrum, sp^{2} carbons were detected. In the ^{13}C NMR spectrum, signals in the range of 30–45 ppm, which correspond to aliphatic (sp^{3}) carbon atoms, and signals from 100–185 ppm, which are indicative of sp^{2} carbon atoms, were observed. Signals in the range of 170–185 ppm, which correspond to carboxyl/amide groups, were also present.[6] In the FTIR analysis of CDs, the following were observed: stretching vibrations of C–OH at 3430 cm^{-1} and C–H at 2923 cm^{-1} and 2850 cm^{-1}, asymmetric stretching vibrations of C-NH-C at 1126 cm^{-1}, bending vibrations of N–H at 1570 cm^{-1}, and the vibrational absorption band of C=O at 1635 cm^{-1} (Figure S5).[7–8] Moreover, the surface groups were also investigated by XPS analysis (Figure 1d). C1s analysis revealed three different types of carbon atoms: graphitic or aliphatic (C=C and C–C), oxygenated, and nitrous (Table S1).[29]

In the UV/Vis spectra, the peak was focused on 344 nm in an aqueous solution of CDs. In the fluorescence spectra, CDs have optimal excitation and emission wavelengths at 360 nm and 443 nm, and show a blue color under a hand-held UV lamp (Figure 2a). Excitation-dependent PL behavior was

---

[*] S. Zhu, Q. Meng, Prof. J. Zhang, Y. Song, Prof. K. Zhang, Prof. B. Yang
State Key Laboratory of Supramolecular Structure and Materials, College of Chemistry, Jilin University
Changchun, 130012 (P. R. China)
E-mail: byangchem@jlu.edu.cn

L. Wang, Prof. H. Wang
State Key Laboratory on Integrated Optoelectronics, College of Electronic Science & Engineering, Jilin University
Changchun, 130012 (P. R. China)

H. Jin, Prof. H. Sun
School of Stomatology, Jilin University
Changchun, 130041 (P. R. China)

[**] This work was supported by the National Science Foundation of China (21221063, 91123031, 50973039, 30830108, 81271111, 21222406) and the National Basic Research Program of China (2012CB933800).

Supporting information for this article is available on the WWW under http://dx.doi.org/10.1002/anie.201300519.

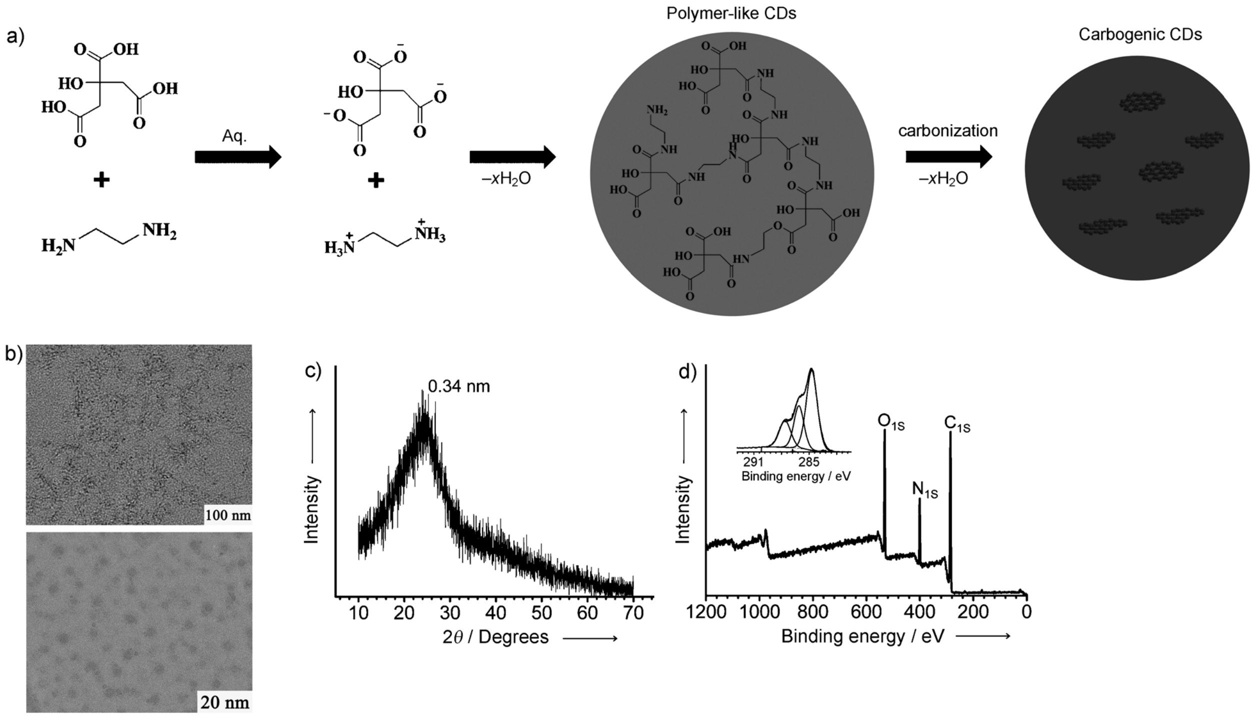

Figure 1. a) A synthetic route using citric acid and ethylenediamine: from ionization to condensation, polymerization, and carbonization. b) TEM (upper) and high-resolution TEM (lower) images of the CDs. c) XRD pattern and d) XPS of CDs.

observed, which is common in fluorescent carbon materials (Figure 2b).[4–8] This behavior is contributed to the surface state affecting the band gap of CDs. The surface state is analogous to a molecular state whereas the size effect is a result of quantum dimensions, both of which contribute to the complexity of the excited states of CDs.[32] Fortunately, excitation-dependent PL behavior can be useful in multicolor imaging applications (Figure S6). Thorough PL quenching was observed in powder samples (Figure S1), which may be attributed to a re-absorption effect, electronic quenching at the excited state, or an induced photothermal effect (Figure S7). Furthermore, the QY of CDs was as high as 60% (using quinine sulfate as a reference); this was even observed under daylight excitation (Figure S8). The PL stability of CDs to the effects of the ionic strength and pH of solutions, and to UV exposure was investigated. There were no changes in photoluminescent intensity or peak characteristics at different ionic strengths (Figure S9a), which is significant because it is necessary for CDs to be used in the presence of physical salt concentrations in practical applications. Another interesting phenomenon is the pH-dependent PL behavior (Figure S9b). PL intensities decrease in a solution of high or low pH, but remain constant in a solution of pH 4–11. However, obvious photobleaching was found after 5 h of continuous UV excitation (Figure S9c). This result may be a consequence of the chemical structure of CDs, most of which have no graphite lattices. The emission control of the surface state/molecule state was strongly affected by surrounding factors, such as solvent pH. At a pH that was too low/high or under exposure to high-power UV radiation, molecular groups are strongly affected.[7,34] It was found to be possible to repeatedly redisperse the dry sample (powder) in water without any aggregation, which is significant for preservation and transportation.

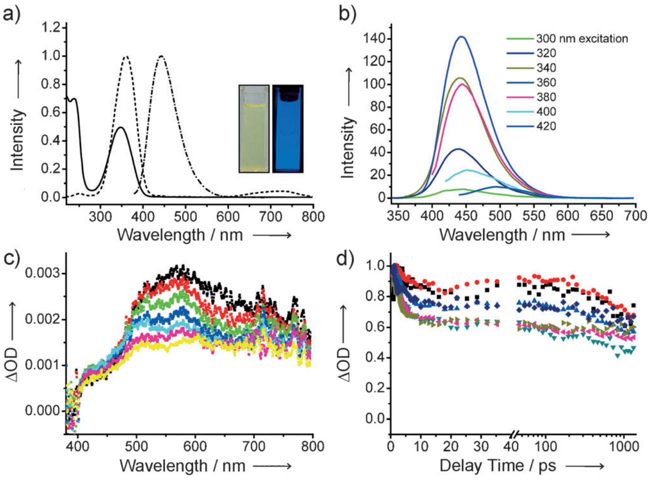

Figure 2. a) UV/Vis absorption (——), PL excitation (-----), and emission (–•–•) spectra of CDs in aqueous solutions (0.05 mg mL^{-1}). Insets show photographs of CDs in aqueous solution under visible (left) and UV (right) light. b) Excitation-dependent PL of CDs. c) TA spectra of CDs. 0.6 ps (black), 2 ps (red), 4 ps (green), 10 ps (dark blue), 100 ps (light blue), 660 ps (pink), 1300 ps (yellow) d) The decay tendency of CDs at different wavelengths. 430 nm (black), 475 nm (red), 510 nm (blue), 555 nm (green), 600 nm (pink), 680 nm (gold), 750 nm (dark blue).

To gain more insight into the origin of the PL behavior, and explain the high QY of CDs, femtosecond broadband (350–800 nm) transient absorption (TA) spectroscopy was performed at 400 nm excitation.[32] From the TA spectra

(Figure 2c,d), the degree of decay is low in all wavelength ranges (less than 50%). During 1300 picosecond intervals, electrons in the excited state retained over 80% activity in the 430–475 nm wavelength range, which subsequently led to radiative fluorescence. This highly stable excited-state is conducive to a high QY.[33] On the other hand, CDs exposed to high-power UV light show drastic decay at all wavelength ranges (excited-state electrons retained only 20% activity), thus leading to a decrease in the QY (Figure S10). The surface-state (molecule) emission plays a leading role in the high luminescence of the CDs, whereas the destruction of the photochemical center after irradiation with high-power UV light gives rise to a decrease in the QY.

The synthetic method can also be used to prepare different CDs by tuning the reaction conditions (Table S2); CDs with a green color can be thus obtained (365 nm excitation). Over many experiments, the OH, COOH, and NH_2 groups were found to be very important for the formation of CDs. First, if the reactants only contained OH and COOH groups, the PL QYs of prepared CDs were always less than 10%. However, if one or more amine groups were present, the PL QYs of most prepared CDs can be over 10% (QY can reach up to 80% under the optimized reaction conditions in Table S2). Citric acid and ethylenediamine were found to be the optimal system for condensation polymerization and further carbonization (Figure 1a). The reaction temperature is also important for CD carbonization (Table S3). As the reaction progressed from low temperature to high temperature, the polymer-like CDs were changed into carbogenic CDs. Figure S13 summarizes the rules determined for temperature effects on CD formation. At low temperature, polymer-like CDs are formed and the PL is due to the surface/molecule state (perhaps owing to amide-containing fluorophores). At high temperature, owing to further carbonization, partial carbogenic CDs are formed and the PL is due to the synergistic effect of the carbogenic core and the surface/molecule state; the carbogenic core plays an ever greater role in the CDs as synthesis temperature increases.

To make use of the high QY, the CDs were utilized in inks for printing patterns. A commercially available paper upon which the CDs adhered well (the paper showed no background UV fluorescence) was chosen as the printing paper. Colorless aqueous solutions of CDs were injected into a vacant cartridge from a commercial inkjet printer. It should be noted that $1\times10^{-3}\,\mathrm{mg\,mL^{-1}}$ of CD ink gave strong enough fluorescence under a UV lamp to be detected.[35] Visible words and images could be observed (Figure 3a). When the concentration of the CDs in the ink was increased, the fluorescence intensity also increased (Figure 3b). In this case, inks with different CD concentrations could serve as different colors for multicolor printing (Figure S14). Furthermore, the CD ink can spread onto hydrophilic strips prepared by photoetching technology. This result has important implications for the use of such inks on a micro scale and for providing multiple colors under UV, blue, and green light excitation (Figure 3c). We also prepared nanocomposites by processing CDs with certain polymers; for example, polyvinyl alcohol (PVA)/CD nanofibers by electrospinning (Figure 3d), and bulk poly *N*,*N*′-dimethylacrylamide (PDMAA)/CD nanocomposites by polymerizing CDs in a DMAA solution (Figure 3e). The stability of the PL to UV light was stronger for CDs in the solid state or in nanocomposites than in solution. The PL intensity remained constant during prolonged UV exposure (Figure S15). Moreover, the printed patterns and prepared nanocomposites retained their stability after four months in an indoor environment, which is beneficial for practical applications.

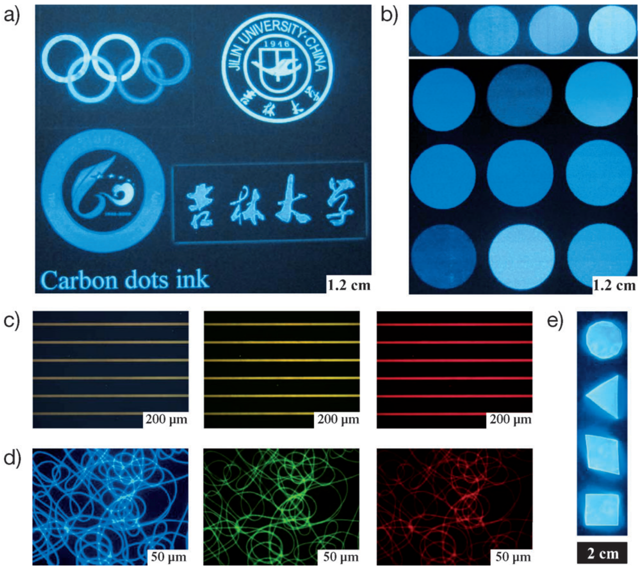

Figure 3. Printed patterns obtained by CD ink and the integration of CDs and polymers. a) Different graphic patterns on paper (illuminated by a portable UV lamp). b) Inks in multiple colors, tuned by the CD concentration in aqueous solution (illuminated by a portable UV lamp). c) CD ink patterned on hydrophilic photoetching stripes (under UV, blue, and green light excitation). d) Fluorescence microscopy images of PVA/CD nanofibers with UV, blue, and green light excitation. The fluorescence microscopy images in (c) and (d) were obtained through band-pass filters of different wavelengths: 450 nm, 550 nm, and 580 nm. e) Bulk PDMAA/CD nanocomposites (The PL intensity was unchanged after 2000 W UV exposure for 30 min).

The fluorescence of the CDs could be quenched by Fe^{3+} ions, because of the special coordination interaction between Fe^{3+} ions and the phenolic hydroxy groups of the CDs, which has been widely used for the detection of Fe^{3+} ions or colored reactions in traditional organic chemistry.[36,37] Fluorescence quenching may contribute to nonradiative electron-transfer that involves partial transfer of an electron in the excited state to the d orbital of Fe^{3+} (Figure S16).[37] To get further insight into the PL quenching mechanism, time-correlated single-photon counting (TCSPC) was used to study the exciton behavior of CDs in the presence and absence of Fe^{3+} (Figure S17). The decay time of CDs is 13.7 ns and has two components: 42.3 ns (ca. 17%) and 7.9 ns (ca. 83%). After coordination with Fe^{3+} ions, the CD/Fe^{3+} decay time decreased to 2.3 ns. Moreover, the fast decay component increased sharply: 7.8 ns (ca. 20%) and 0.9 ns (ca. 80%). The significantly reduced lifetime indicates an ultrafast CD/Fe^{3+} electron-transfer process and leads to dynamic quenching. Figure 4a shows the fluorescent quenching value of CDs with varying concentrations of Fe^{3+} ions. The detection limit was

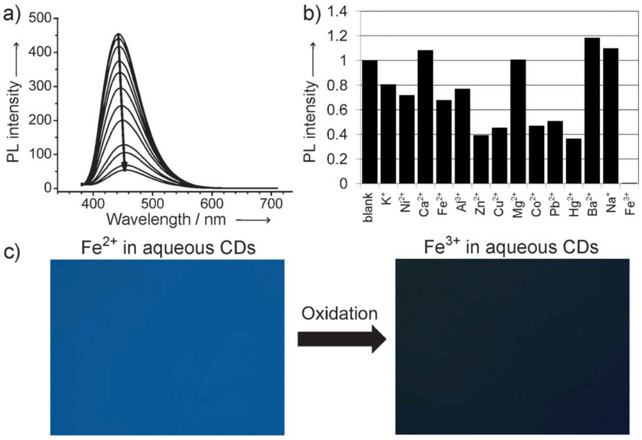

Figure 4. a) Fluorescence quenching in the presence of Fe^{3+} ions (0–300 ppm). Downward-pointing arrow shows the trend as the concentration of Fe^{3+} ions increases. b) Comparison of fluorescence intensities of CDs after the addition of different metal ions. c) Fluorescence images of aqueous CDs after adding Fe^{2+} and Fe^{3+} ions. The on/off fluorescence was achived by oxidation.

calculated to be around 1 ppm. Furthermore, we investigated the fluorescence quenching effect of various metal ions on CDs: different metal ions (K^+, Ni^{2+}, Ca^{2+}, Fe^{2+}, Al^{3+}, Zn^{2+}, Cu^{2+}, Mg^{2+},Co^{2+}, Pb^{2+}, Hg^{2+}, Ba^{2+}, Na^+, and Fe^{3+}), each at a concentration of 10^{-2} mol L^{-1}, were added into a CD dispersion (0.001 mg mL^{-1}; Figure 4b). Fe^{3+} ions had the greatest effect on fluorescence quenching among the metal ions tested. For Fe^{2+}, Zn^{2+}, Cu^{2+}, Co^{2+}, Pb^{2+}, and Hg^{2+} ions, the slight fluorescence quenching can be attributed to the nonspecific interactions between the carboxylic groups and the metal ions.[37] Moreover, the on/off fluorescence in such an imaging system with Fe^{2+}/Fe^{3+} medium could be achived by oxidation (Figure 4c). Fe^{3+} ions are indispensable for a large number of living systems, and play an important role in many biochemical processes. The detection of Fe^{3+} ions through a visible fluorescent method, would be of considerable benefit. An MTT assay showed that the CDs possess low cytotoxicity, and thus could act as an excellent bioimaging reagent (Figure S18). As expected, after incubating with a CD-culture solution, the fluorescence in the cells retained a high intensity, and the excitation-dependent PL resulted in multicolor imaging under different excitation wavelengths (Figure S19). Moreover, the PL intensity changed to a certain degree after the addition of 0.1 mM Fe^{2+} and 0.1 mM Fe^{3+} in the incubation medium (Figure S20).

In summary, a facile and high-output method for the fabrication of CDs with a QY as high as ca. 80% was developed. The chemical structure and PL mechanism were investigated in detail. The polymer-like CDs were changed into carbogenic CDs through a low-to-high temperature synthesis. The surface/molecule state plays the leading role in the polymer-like CDs, whereas the synergistic effect of the carbon core and the surface/molecule state contributed to the PL of carbogenic CDs. Moreover, the CDs were applied both as printing inks, which are capable of producing multicolor patterns on the microscale, and as functional nanocomposites that could potentially be used in anti-counterfeit applications. Furthermore, the CDs could be utilized as a biosensor reagent capable of detecting Fe^{3+} in biosystems. Some questions still remain to be addressed, such as the exact chemical identities of the CDs, especially whenever nanoparticles are formed with alterative synthesis temperatures.[5]

Received: January 21, 2013

Keywords: bioimaging · carbon · nanomaterials · photoluminescence

---

[1] a) L. Cao, M. J. Meziani, S. Sahu, Y. P. Sun, *Acc. Chem. Res.* **2013**, *46*, 171–180; b) S. N. Baker, G. A. Baker, *Angew. Chem.* **2010**, *122*, 6876–6896; *Angew. Chem. Int. Ed.* **2010**, *49*, 6726–6744; c) H. Li, Z. Kang, Y. Liu, S. T. Lee, *J. Mater. Chem.* **2012**, *22*, 24230–24253.
[2] Y. Fang, S. Guo, D. Li, C. Zhu, W. Ren, S. Dong, E. Wang, *ACS Nano* **2012**, *6*, 400–409.
[3] X. Wang, L. Cao, S. T. Yang, F. Lu, M. J. Meziani, L. Tian, K. W. Sun, M. A. Bloodgood, Y. P. Sun, *Angew. Chem.* **2010**, *122*, 5438–5442; *Angew. Chem. Int. Ed.* **2010**, *49*, 5310–5314.
[4] R. Liu, D. Wu, S. Liu, K. Koynov, W. Knoll, Q. Li, *Angew. Chem.* **2009**, *121*, 4668–4671; *Angew. Chem. Int. Ed.* **2009**, *48*, 4598–4601.
[5] M. J. Krysmann, A. Kelarakis, P. Dallas, E. P. Giannelis, *J. Am. Chem. Soc.* **2012**, *134*, 747–750.
[6] H. Liu, T. Ye, C. Mao, *Angew. Chem.* **2007**, *119*, 6593–6595; *Angew. Chem. Int. Ed.* **2007**, *46*, 6473–6475.
[7] X. Zhai, P. Zhang, C. Liu, T. Bai, W. Li, L. Dai, W. Liu, *Chem. Commun.* **2012**, *48*, 7955–7957.
[8] D. Pan, J. Zhang, Z. Li, C. Wu, X. Yan, M. Wu, *Chem. Commun.* **2010**, *46*, 3681–3683.
[9] H. Li, X. He, Z. Kang, H. Huang, Y. Liu, J. Liu, J. Liu, S. Lian, C. H. A. Tsang, X. Yang, S. T. Lee, *Angew. Chem.* **2010**, *122*, 4532–4536; *Angew. Chem. Int. Ed.* **2010**, *49*, 4430–4434.
[10] L. Bao, Z. L. Zhang, Z. Q. Tian, L. Zhang, C, Liu, Y. Lin, B. Qi, D. W. Pang, *Adv. Mater.* **2011**, *23*, 5801–5806.
[11] B. Kong, A. Zhu, C. Ding, X. Zhao, B. Li, Y. Tian, *Adv. Mater.* **2012**, *24*, 5844–5848.
[12] A. Krueger, *Adv. Mater.* **2008**, *20*, 2445–2449.
[13] K. Welsher, Z. Liu, S. P. Sherlock, J. T. Robinson, Z. Chen, D. Daranciang, H. Dai, *Nat. Nanotechnol.* **2009**, *4*, 773–780.
[14] J. Jeong, M. Cho, Y. T. Lim, N. W. Song, B. H. Chung, *Angew. Chem.* **2009**, *121*, 5400–5403; *Angew. Chem. Int. Ed.* **2009**, *48*, 5296–5299.
[15] K. P. Loh, Q. Bao, G. Eda, M. Chhowalla, *Nat. Chem.* **2010**, *2*, 1015–1024.
[16] a) S. Zhu, S. Tang, J. Zhang, B. Yang, *Chem. Commun.* **2012**, *48*, 4527–4539; b) S. Zhu, J. Zhang, C. Qiao, S. Tang, Y. Li, W. Yuan, B. Li, L. Tian, F. Liu, R. Hu, H. Gao, H. Wei, H. Zhang, H. Sun, B. Yang, *Chem. Commun.* **2011**, *47*, 6858–6860; c) S. Zhu, J. Zhang, X. Liu, B. Li, X. Wang, S. Tang, Q. Meng, Y. Li, C. Shi, R. Hu, B. Yang, *RSC Adv.* **2012**, *2*, 2717–2720.
[17] S. Zhu, J. Zhang, S. Tang, C. Qiao, L. Wang, H. Wang, X. Liu, B. Li, Y. Li, W. Yu, X. Wang, H. Sun, B. Yang, *Adv. Funct. Mater.* **2012**, *22*, 4732–4740.
[18] S. Zhuo, M. Shao, S. T. Lee, *ACS Nano* **2012**, *6*, 1059–1064.
[19] V. Gupta, N. Chaudhary, R. Srivastava, G. D. Sharma, R. Bhardwaj, S. Chand, *J. Am. Chem. Soc.* **2011**, *133*, 9960–9963.
[20] X. Feng, V. Marcon, W. Pisula, M. R. Hansen, J. Kirkpatrick, F. Grozema, D. Andrienko, K. Kremer, K. Müllen, *Nat. Mater.* **2009**, *8*, 421–426.
[21] X. Yan, X. Cui, L. Li, *J. Am. Chem. Soc.* **2010**, *132*, 5944–5945.

[22] J. Wang, C. F. Wang, S. Chen, *Angew. Chem.* **2012**, *124*, 9431 – 9435; *Angew. Chem. Int. Ed.* **2012**, *51*, 9297 – 9301.

[23] S. Qu, X. Wang, Q. Lu, X. Liu, L. Wang, *Angew. Chem.* **2012**, *124*, 12381 – 12384; *Angew. Chem. Int. Ed.* **2012**, *51*, 12215 – 12218.

[24] F. Wang, Z. Xie, H. Zhang, C. Liu, Y. Zhang, *Adv. Funct. Mater.* **2011**, *21*, 1027 – 1031.

[25] Z. C. Yang, M. Wang, A. M. Yong, S. Y. Wong, X. H. Zhang, H. Tan, A. Y. Chang, X. Li, J. Wang, *Chem. Commun.* **2011**, *47*, 11615 – 11617.

[26] Y. Yang, J. Cui, M. Zheng, C. Hu, S. Tan, Y. Xiao, Q. Yang, Y. Liu, *Chem. Commun.* **2012**, *48*, 380 – 382.

[27] C. Zhu, J. Zhai, S. Dong, *Chem. Commun.* **2012**, *48*, 9367 – 9369.

[28] S. Sahu, B. Behera, T. K. Maiti, S. Mohapatra, *Chem. Commun.* **2012**, *48*, 8835 – 8837.

[29] S. Liu, J. Tian, L. Wang, Y. Zhang, X. Qin, Y. Luo, A. M. Asiri, A. O. A-Youbi, X. Sun, *Adv. Mater.* **2012**, *24*, 2037 – 2041.

[30] X. Jia, J. Li, E. Wang, *Nanoscale* **2012**, *4*, 5572 – 5575.

[31] X. Zhang, S. Wang, L. Xu, L. Feng, Y. Ji, L, Tao, S. Li, Y. Wei, *Nanoscale* **2012**, *4*, 5581 – 5584.

[32] J. Shang, L. Ma, J. Li, W. Ai, T. Yu, G. G. Gurzadyan, *Sci. Rep.* **2012**, *2*, 792.

[33] a) J. R. Lakowicz, *Principles of Fluorescence Spectroscopy*, 3rd ed., Springer, New York, **2006**; b) S. Zhu, J. Zhang, L. Wang, Y. Song, G. Zhang, B. Yang, *Chem. Commun.* **2012**, *48*, 10889 – 10891.

[34] Y. Dong, J. Shao, C. Chen, H. Li, R. Wang, Y. Chi, X. Lin, G. Chen, *Carbon* **2012**, *50*, 4738 – 4743.

[35] Q. Mei, Z. Zhang, *Angew. Chem.* **2012**, *124*, 5700 – 5704; *Angew. Chem. Int. Ed.* **2012**, *51*, 5602 – 5606.

[36] D. Wang, L, Wang, X. Dong, Z. Shi, J. Jin, *Carbon* **2012**, *50*, 2147 – 2154.

[37] E. F. Wesp, W. R. Brode, *J. Am. Chem. Soc.* **1934**, *56*, 1037 – 1042.